Chin. Geogra. Sci. 2022 Vol. 32 No. 5 pp. 824−833
https://doi.org/10.1007/s11769-022-1303-3

Springer Science Press
www.springerlink.com/content/1002-0063

Lockdown-induced Urban Aerosol Change over Changchun, China During COVID-19 Outbreak with Polarization LiDAR

CHEN Weiwei[1], DUANMU Lingjian[1, 2], QIN Yang[3], YANG Hongwu[4], FU Jing[1], LU Chengwei[5], FENG Wei[6], GUO Li[2]

(1. *Key Laboratory of Wetland Ecology and Environment*, *Northeast Institute of Geography and Agroecology*, *Chinese Academy of Sciences*, *Changchun* 130102, *China*; 2. *College of Biological and Agricultural Engineering*, *Jilin University*, *Changchun* 130022, *China*; 3. *Jilin Provincial Ecological Environment Monitoring Center*, *Changchun* 130012, *China*; 4. *Hongke Photonics Company*, *Liaoyuan* 136200, *China*; 5. *The Department of Ophthalmology*, *The First Hospital of Jilin University*, *Changchun* 130021, *China*; 6. *Key Lab of Groundwater Resources and Environment*, *Jilin University*, *Changchun* 130021, *China*)

Abstract: Depending on various government policies, COVID-19 (Corona Virus Disease-19) lockdowns have had diverse impacts on global aerosol concentrations. In 2022, Changchun, a provincial capital city in Northeast China, suffered a severe COVID-19 outbreak and implemented a very strict lockdown that lasted for nearly two months. Using ground-based polarization Light Detection and Ranging (LiDAR), we detected real-time aerosol profile parameters (EC, extinction coefficient; DR, depolarization ratio; AOD, aerosol optical depth), as well as air-quality and meteorological indexes from 1 March to 30 April in 2021 and 2022 to quantify the effects of lockdown on aerosol concentrations. The period in 2022 was divided into three stages: pre-lockdown (1−10 March), strict lockdown (11 March to 10 April), and partial lockdown (11–30 April). The results showed that, during the strict lockdown period, compared with the pre-lockdown period, there were substantial reductions in aerosol parameters (EC and AOD), and this was consistent with the concentrations of the atmospheric pollutants $PM_{2.5}$ (particulate matter with an aerodynamic diameter ≤ 2.5 μm) and PM_{10} (particulate matter with an aerodynamic diameter ≤ 10 μm), and the O_3 concentration increased by 8.3%. During the strict lockdown, the values of EC within 0–1 km and AOD decreased by 16.0% and 11.2%, respectively, as compared to the corresponding period in 2021. Lockdown reduced the conventional and organized emissions of air pollutants, and it clearly delayed the time of seasonal emissions from agricultural burning; however, it did not decrease the number of farmland fire points. Considering meteorological factors and eliminating the influence of wind-blown dust events, the results showed that reductions from conventional organized emission sources during the strict lockdown contributed to a 30% air-quality improvement and a 22% reduction in near-surface extinction (0–2 km). Aerosols produced by urban epidemic prevention and disinfection can also be identified using the EC. Regarding seasonal sources of agricultural straw burning, the concentrated burning induced by the epidemic led to the occurrence of heavy pollution from increased amounts of atmospheric aerosols, with a contribution rate of 62%. These results indicate that there is great potential to further improve air quality in the local area, and suggest that the comprehensive use of straw accompanied by reasonable planned burning is the best way to achieve this.

Keywords: $PM_{2.5}$ (particulate matter with an aerodynamic diameter ≤ 2.5 μm); NO_2; O_3; aerosol optical depth (AOD); extinction coefficient; depolarization ratio; COVID-19 (Corona Virus Disease-19) lockdown

Citation: CHEN Weiwei, DUANMU Lingjian, QIN Yang, YANG Hongwu, FU Jing, LU Chengwei, FENG Wei, GUO Li, 2022. Lockdown-induced Urban Aerosol Change over Changchun, China During COVID-19 Outbreak with Polarization LiDAR. *Chinese Geographical Science*, 32(5): 824−833. https://doi.org/10.1007/s11769-022-1303-3

Received date: 2022-06-07; accepted date: 2022-07-12

Foundation item: the Key Research Program of Frontier Sciences, Chinese Academy of Sciences (No. QYZDB-SSW-DQC045), the National Natural Science Foundation of China (No. 41775116)

Corresponding author: CHEN Weiwei. E-mail: chenweiwei@neigae.ac.cn; GUO Li. E-mail: liguo2012@jlu.edu.cn

1 Introduction

In March and April 2022, Changchun, a provincial capital city in Northeast China, experienced the worst COVID-19 (Corona Virus Disease-19) outbreak. Subsequently, the government declared mandatory preventive isolation, dynamically classified the risk levels of the epidemic in the region, formulated corresponding administrative lockdown measures, closed all kinds of enterprises (except livelihood-protection enterprises), kept residents at home, and carried out a number of city-wide disinfections to prevent cross-infection and try to control the spread of COVID-19 (Liu et al., 2022). This strict lockdown period was last from 11 Mach to 10 April. Subsequently, the epidemics was under control and the government resumed the transport industry and some business producing essential goods, and the citizens were allowed walk around within their community (11−30 April), called as partial lockdown. Such a long-term administrative lockdown provides a good case study for research on possible further improvements to air quality in cities in Northeast China. This includes the response of aerosol parameters to epidemic changes, assessment of the maximum potential air quality, and the contributions of anthropogenic emission sources (Collivignarelli et al., 2020; Nakada and Urban, 2020; Benchrif et al., 2021). Herein, using multisource data (including aerosol LiDAR (Light Detection and Ranging), satellite data, air-quality indexes, and meteorological parameters), for the first time, we report the characteristics and main causes of air-quality and aerosol changes during the epidemic period of Changchun, Northeast China.

2 Materials and Methods

Multisource hourly data, including satellite-based fire points, air-quality indexes ($PM_{2.5}$ (particulate matter with an aerodynamic diameter ≤ 2.5 μm), PM_{10} (particulate matter with an aerodynamic diameter ≤ 10 μm), SO_2, NO_2, CO, and O_3), aerosol optical depth (AOD) at 532 nm, meteorological parameters (planetary boundary-layer height: PBLH, air temperature, relative humidity, precipitation, wind speed, and wind direction) in study period (1 March to 30 April in 2021 and 2022) and LiDAR-based aerosol profile parameters (EC (extinction coefficient), DR (depolarization ratio)) during pre-lockdown (1–10 March), strict lockdown (11 March to 10 April), and partial lockdown (11–30 April), were analyzed for the evaluation of aerosol changes in the counterpart periods of 2021 and 2022.

At the Northeast Institute of Geography and Agroecology, Chinese Academy of Sciences in Changchun City (44°00′N, 125°24′E), we installed a ground-based polarized LiDAR with a 532-nm wavelength laser launcher produced by Jilin Hongke Photonics Corporation (HK-LiDAR-V-1000), and obtained the data of aerosol parameters detected during the study period. The maximum pump-pulse energy of this system is 12 mJ, the range resolution is 7.5 m, it has an interval operating time of 20 s, and its detection blind area is 200–300 m. The DR is defined as the ratio of the return signal in a perpendicular to parallel polarization relative to the outgoing laser light (Murayama et al., 1999).

The profiles of aerosol EC were derived using the inversion algorithm of Fernald (1984), which holds that aerosols and atmospheric molecules make up the atmosphere together. The value of the AOD at 532 nm can then be obtained from the integral of the EC (Gobbi et al., 2000). The PBLH was calculated using the gradient method based on LiDAR data. Daily straw-burning fire points information was detected by Earth Observing System AM-1 satellite named Terra, Earth Observing System PM-1 satellite named Aqua and National Polar-orbiting Partnership (NPP), and the data were obtained from the Fire Information for Resource Management System (https://firms.modaps.eosdis.nasa.gov/). Hourly measurements of the urban air-quality index (AQI), meteorological parameters, and atmospheric pollutants (PM_{10}, $PM_{2.5}$, SO_2, NO_2, CO, and O_3) in Changchun City were provided by the Environmental Monitoring Center of Jilin Province. Relative changes in these indexes among various stage of lockdown periods in 2021 and 2022 were analyzed using the R software package (Lu et al., 2021).

3 Results and Discussion

In the Northeast China Plain, spring is a period in which air pollution is typically the result of three main types of emission source (Li et al., 2020). The first is conventional emission sources of atmospheric pollutants from production and daily life, including industrial, mobile, and other residential sources. The second is coal com-

bustion, because March and April are still in the period where heating of buildings is required. The third and final source is soil erosion and agriculture, which are seasonal emission sources. With increasing wind speeds and the melting of snow, bare desert and farmland soil can easily form natural wind-blown dust. At the same time, extensive agricultural activities in spring and open burning of straw will increase the air-pollution levels during this period (Shen et al., 2007; Chen et al., 2017). Under the current straw-burning control policy, straw-burning activities increase significantly in spring. During the strict lockdown period, industrial, mobile, commercial cooking, and agricultural sources of air-pollution emissions were drastically reduced. Previous studies have shown that the strict lockdowns in Wuhan and Beijing caused almost industry-wide stagnation and resulted in significant air-quality improvements (Lian et al., 2020; Hua et al., 2021). During the partial lockdown period (11 April to 30 April), essential industry sources gradually recovered, and agricultural farming activities and biomass burning were again carried out on a large scale.

To assess the impact of human-induced lockdowns on air quality and aerosols, it is necessary to eliminate interference from natural sources. Over 1 March to 30 April in 2021 and 2022, the daily air temperature, relative humidity, and wind speed ranged from −12°C−19.6°C, 21.2%−97.6%, and 1.2−7.6 m/s, respectively (Table 1). During this period, the cumulative mean daily precipitation varied from 10.1 to 18.1 mm, with a maximum of 155.8 mm on 22 April 2022. In addition, atmospheric visibility was within the ranges

Table 1 Meteorological parameters, air pollutants, aerosol prosperities, and their relative changes for different periods of COVID-19 lockdown in 2022 in Changchun City, China

Parameter	Year	Pre-lockdown				Strict lockdown				Partial lockdown				Whole period			
		Mean	Min	Max	RC / %	Mean	Min	Max	RC / %	Mean	Min	Max	RC / %	Mean	Min	Max	RC / %
T_a / °C	2021	−2.4	−12.0	5.7	–	6.1	−1.8	14.2	–	10.1	2.0	19.6	–	6.0	−12.0	19.6	–
	2022	−0.2	−4.3	7.0	–	3.2	−8.0	16.7	–	11.2	3.4	19.2	–	5.3	−8.0	19.2	–
Precipitation / mm	2021	6.7	0.0	43.6	–	6.4	0.0	101.4	–	17.5	0.0	106.7	–	10.1	0.0	106.7	–
	2022	1.9	0.0	16.3	−72.1	21.4	0.0	150.3	232.1	20.1	0.0	155.8	14.9	18.1	0.0	155.8	78.5
RH / %	2021	52.6	36.0	69.7	–	48.3	21.2	97.6	–	46.1	21.5	87.4	–	48.3	21.2	97.6	–
	2022	47.1	32.6	70.6	−10.4	52.4	25.3	90.5	8.5	44.0	25.0	83.5	−4.5	48.4	25.0	90.5	0.3
WS / (m/s)	2021	3.4	1.7	5.8	–	3.0	1.2	5.6	–	3.3	1.6	5.4	–	3.2	1.2	5.8	–
	2022	3.3	1.5	6.0	−2.6	3.5	1.6	7.6	16.8	3.8	1.9	6.9	14.4	3.6	1.5	7.6	12.5
Visibility / km	2021	18.0	8.4	30.0	–	11.6	4.8	19.6	–	11.6	7.0	14.9	–	12.6	4.8	30.0	–
	2022	14.2	7.0	21.6	−21.4	15.0	4.5	24.1	29.8	14.8	7.2	24.5	27.5	14.9	4.5	24.5	18.1
PM_{10} / (μg/m^3)	2021	70.3	32.0	116.0	–	108.0	29.0	258.0	–	83.7	20.0	161.0	–	93.9	20.0	258.0	–
	2022	75.6	26.0	139.0	7.5	55.7	20.0	275.0	−48.4	85.9	13.0	276.0	2.6	67.1	13.0	276.0	−28.5
$PM_{2.5}$ / (μg/m^3)	2021	42.9	18.0	78.0	–	52.7	12.0	141.0	–	37.6	10.0	85.0	–	46.1	10.0	141.0	–
	2022	37.0	13.0	76.0	−13.8	31.0	9.0	122.0	−41.2	50.3	9.0	139.0	33.7	37.1	9.0	139.0	−19.5
NO_2 / (μg/m^3)	2021	35.0	19.0	47.0	–	39.2	19.0	68.0	–	30.1	14.0	46.0	–	35.5	14.0	68.0	–
	2022	29.8	13.0	47.0	−14.9	15.1	8.0	24.0	−61.3	11.0	4.0	34.0	−63.6	15.6	4.0	47.0	−56.1
O_3 / (μg/m^3)	2021	79.0	67.0	100.0	–	93.1	40.0	148.0	–	102.3	57.0	174.0	–	93.8	40.0	174.0	–
	2022	81.3	69.0	107.0	2.9	100.8	54.0	159.0	8.3	123.2	78.0	163.0	20.5	104.5	54.0	163.0	11.4
AOD	2021	0.3	0.1	0.8	–	0.3	0.1	0.7	–	0.4	0.2	0.8	–	0.4	0.1	0.8	–
	2022	0.4	0.1	0.8	6.6	0.3	0.1	0.7	−11.2	0.4	0.2	0.6	−16.0	0.3	0.1	0.8	−10.4
PBLH / km	2021	1.3	0.7	2.2	–	1.6	0.7	2.7	–	1.6	0.9	2.3	–	1.6	0.7	2.7	–
	2022	1.5	0.7	2.4	20.9	1.7	0.4	2.6	4.3	1.6	0.8	2.8	−0.8	1.6	0.4	2.8	5.3

Notes: T_a: air temperature; RH: relative humidity; WS: wind speed; AOD: aerosol optical depth; PBLH: planetary boundary-layer height; RC: relative change of each parameter in 2022 as compared to 2021. pre-lockdown, strict lockdown, and partial lockdown represent the periods 1–10 March, 11 March to 10 April, and 11–30 April in 2021 and 2022, respectively

4.8–30.0 km in 2021 and 4.5–24.5 km in 2022. In March to April in 2022, there was an increase in accumulated precipitation of 78.5% (8.1 mm), nearly identical relative humidity, an increase in visibility of 18.1% (2.6 km), and an increase in wind speed of 12.5% (0.4 m/s) compared to the same period in 2021. He et al. (2017) studied meteorological parameters in the Northeastern region of China during 2014–2015, and found that an increase in wind speed can facilitate atmospheric dispersion, which improved visibility. Therefore, the changes in meteorological conditions in 2022 could have mitigated atmospheric pollution to some extent compared to the previous year. However, more 'dust days' occurred in 2022 (24, 28 and 29 March and 3, 4, 7, 9, 10, 19, 20, 21, 23, 25, 26 and 30 April) than in 2021 (15, 26, 27, 28 and 29 March and 2, 27 and 28 April). As the Gobi Desert, the Ortindag Sands, and the Kerchin Sands are located in the western part of Northeast China, the frequent westerly winds in spring increase the occurrence of dust and wind erosion of agricultural land in the Northeast (Wang et al., 2004; Wang et al., 2010; Zhao et al., 2022). Therefore, in 2022, compared with the previous year, greater emissions of coarse particulate matter in spring were caused by natural conditions.

As can be seen from the Table 1, the lockdown significantly reduced the concentrations of particulate matter ($PM_{2.5}$ and PM_{10}) and NO_2, but it had little effect on the O_3 concentration. During the study period in 2022, daily average concentrations of PM_{10}, $PM_{2.5}$, NO_2, and O_3 varied from 13−276 mg/m^3, 9−139 mg/m^3, 4−47 mg/m^3, and 54−163 mg/m^3, respectively. The concentrations of most atmospheric particulates during the strict lockdown period were lower than those in the pre-lockdown and partial lockdown periods, indicating the significant anthropogenic control of particulate emission sources; some of the higher levels were mainly induced by windblown dust from natural sources. Furthermore, NO_2 concentrations decreased by 49% during the lockdown period as compared to pre-lockdown, indicating a significant reduction of mobile-source emissions. Compared with 2021, the concentrations of atmospheric pollutants during pre-lockdown in 2022 were comparable. The mean concentrations of PM_{10}, $PM_{2.5}$, and NO_2 during strict lockdown significantly decreased, by 48.4%, 41.2%, and 61.3%, respectively. The concentrations of PM_{10} and $PM_{2.5}$ during partial lockdown increased by 2.6% and 33.7%, respectively. However, the concentration of NO_2 decreased by 63.6%. Previous studies have shown that lockdowns have resulted in significant reductions in NO_2 (Barcelona: 48%, New York: 51%, São Paulo: 54%, and 22 cities in India: 18% on average), increases in O_3 (Barcelona: 45%, 22 cities in India: 17%, and São Paulo: 30%) and reductions in $PM_{2.5}$ (New York: 36%, 22 cities in India: 43% on average) (Nakada and Urban, 2020; Sharma et al., 2020; Tobías et al., 2020; Zangari et al., 2020). Compared to other regions of the world, NO_2 (Wuhan: 53%, Beijing: 60%) and $PM_{2.5}$ (Wuhan: 36%, Beijing: 35%) were reduced significantly due to the strict lockdown in China (Lian et al., 2020; Hua et al., 2021). Thus, with the support of the strictest lockdown conditions, this study effectively examined the maximum potential improvement of air quality in the Changchun area.

During the first 10 d of the partial lockdown period, the concentrations of atmospheric particulates in 2022 were significantly higher than those in the same period of 2021, and the concentration of NO_2 was lower (Fig. 1). According to the variations in the fire points, straw burning was concentrated in two periods (25–31 March and 15–18 April) in 2021, while in 2022 it was mainly in the period 13–18 April, as shown in Fig. 1. Due to the long duration of winter in Northeast China and the impact of government straw restrictions, straw used to be burned in the spring, i.e., within March and April (Fu et al., 2022). However, because farmers were allowed to return villages for farming, this resulted in an obvious increase in air-pollutant emissions with the increase of straw burning and the activities of agricultural machinery.

As shown in Fig. 1, during the study period, lockdown resulted in a decrease in AOD at 532 nm. The daily means of AOD and PBLH for the study period in 2022 ranged from 0.1 to 0.8 km and 0.4 to 2.8 km, respectively. The PBLH from March to April 2022 increased by 5.3% over the same period in 2021.Compared with 2021, AOD values decreased by 0.0348 (11.2%) in 2022 during the strict lockdown and by 0.0679 (16.0%) during the partial lockdown. According to research by Thomas et al. (2021), the AOD of the Ganges Plain region (India) decreased by 10%–25% during the COVID-19 lockdown period. Due to the strict lockdown, the AOD within the boundary layer declined to half of that of the same period in Wuhan (an

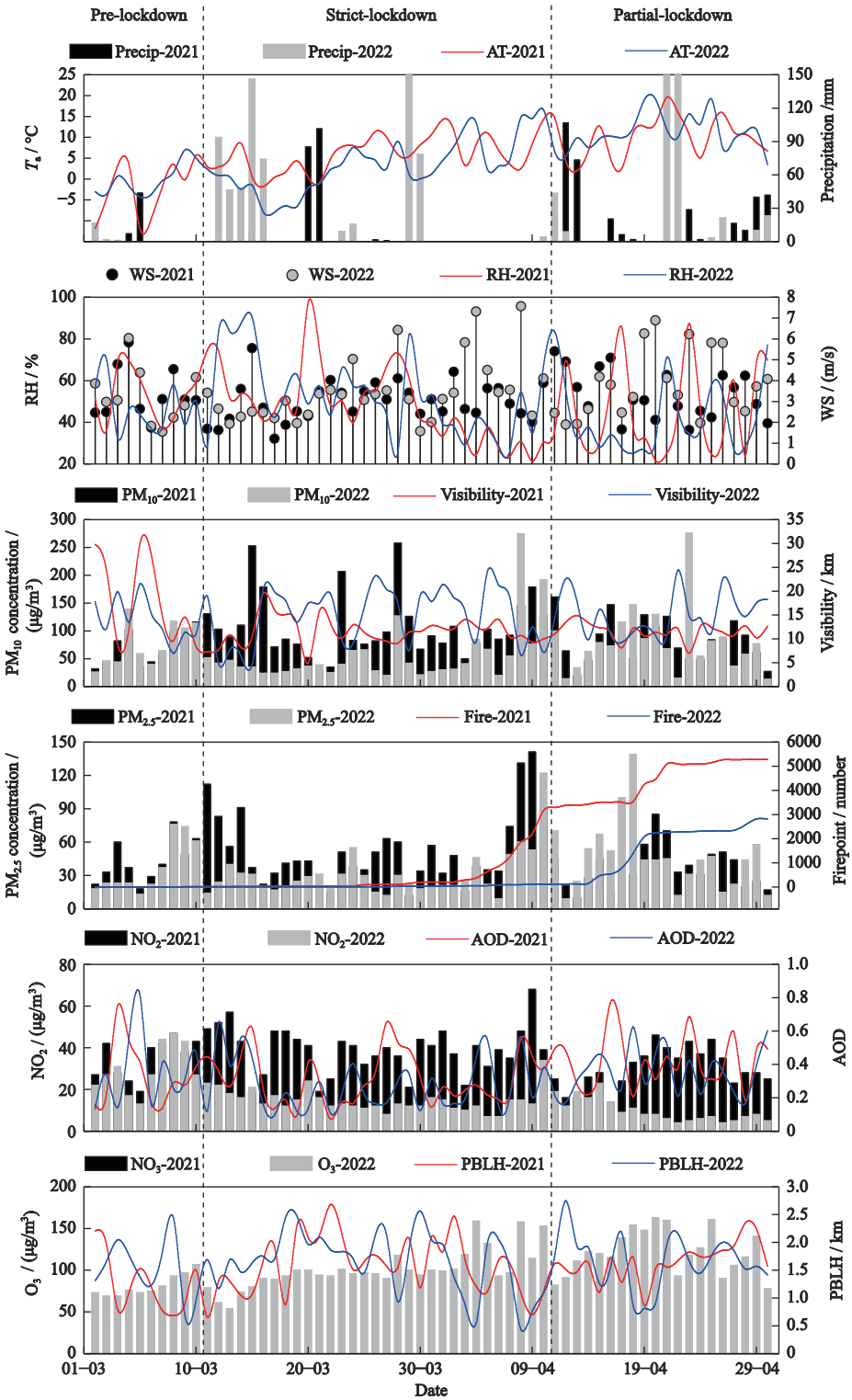

Fig. 1 Temporal variations in meteorological parameters (air temperature (T_a), precipitation, relative humidity (RH), wind speed (WS) and visibility), air pollutants including coarse particulate matter (PM_{10}), fine particulate matter ($PM_{2.5}$), Nitrogen dioxide (NO_2) and ozone (O_3), satellite-based fire points in farmland, ground-layer aerosol properties (aerosol optical depth (AOD) and planetary boundary-layer height (PBLH) in Changchun City, China during different stages of study periods in 2021 and 2022. The whole period from 1 March to 30 April was divided into three main periods: pre-lockdown (1–10 March), strict lockdown (11 March to 11 April) and partial lockdown (12 April to 30 April). In partial lockdown, the practices of agricultural tillage and important living and production enterprises were allowed

important transport hub in China), and it reached a minimum value of 0.125 (Yin et al., 2021). These results confirm that the COVID-19 lockdown resulted in significant changes in aerosol properties within the planetary boundary layer.

Vertical profiles of EC are shown in Fig. 2, in which cloud aerosols, dust aerosols, and smoke aerosols are highlighted by light blue, yellow, and black frames, respectively. There were two incidents of smoke from straw burning in the period 1–11 April 2021, which is the same period defined as strict lockdown in 2022. Long periods of smoke-aerosol pollution events were detected during 8–11 April 2021, while no smoke events were detected during the same period in 2022 due to the

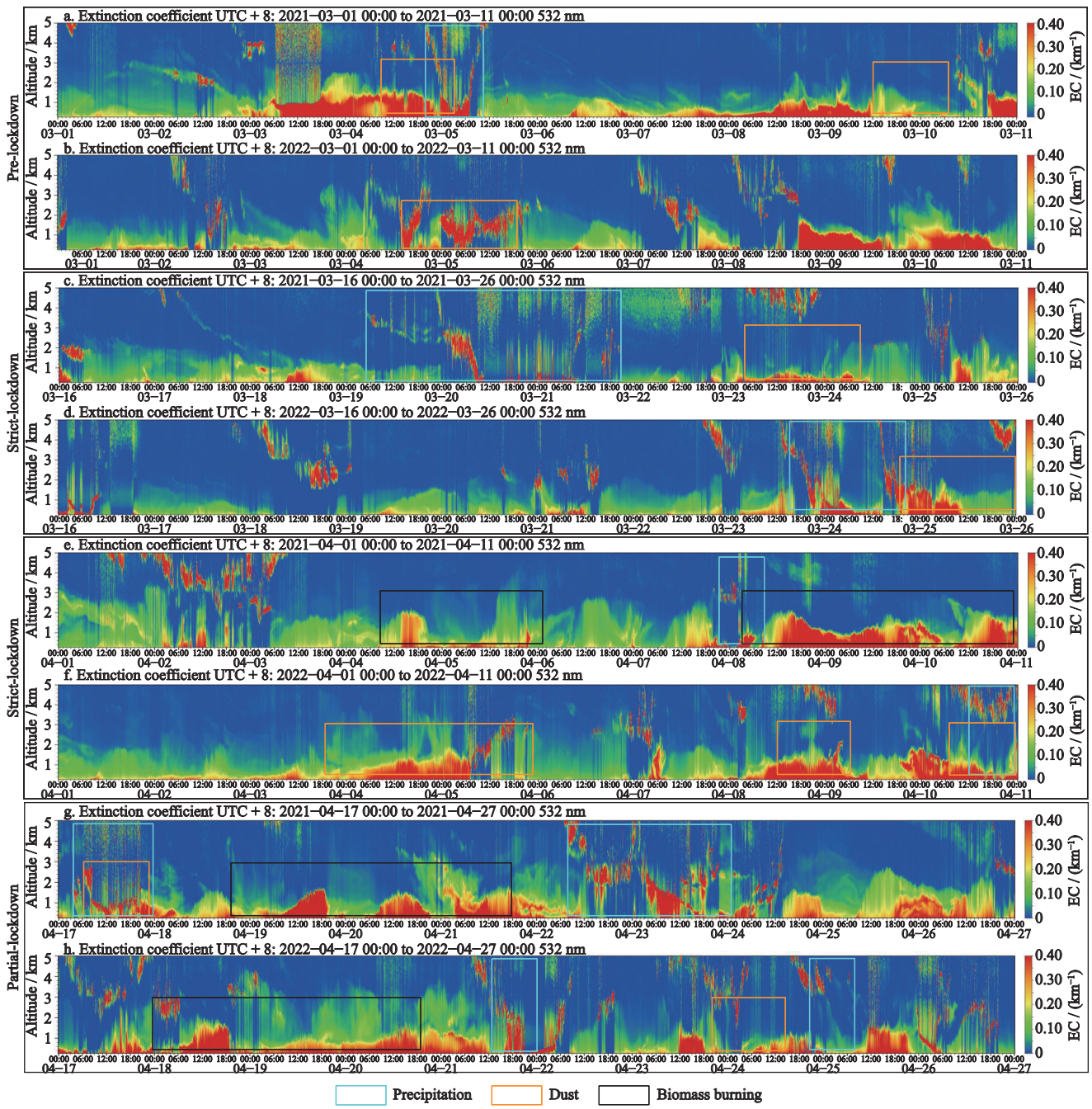

Fig. 2 Vertical profiles of aerosol optical extinction coefficient (EC) at sub-minute scales during different stages of lockdown in Changchun City, China. The period 12–26 March in strict lockdown in 2022 and the corresponding time in 2021 represented no agricultural activities, while agricultural burning occurred in the period of 1–11 April

strict lockdown. However, considering the effects of concentrated straw burning, the EC within 2–4 km during the lockdown period was significantly higher than 0.4 km^{-1}. As reported in a previous study (Bhawar et al., 2021), burning biomass in northern India created an aerosol layer near 2–4 km, but the fires negated the beneficial effects of the government-imposed lockdown in central India. Thus, the straw-burning events that occurred in Changchun 2022 partially offset the impact of the lockdown on aerosols while contributing to the observed increase in $PM_{2.5}$ values.

It can be observed, from the vertical profiles of DR are shown in Figs.3 a, 3b, that the trend of DR variations were similar during pre-lockdown periods in 2021 and 2022. A decreasing trend in DR (Figs. 3c, 3d), however, was evident during the beginning of the strict lockdown period (16 March−26 March) caused by the implementation of the lockdown policies. Besides, A

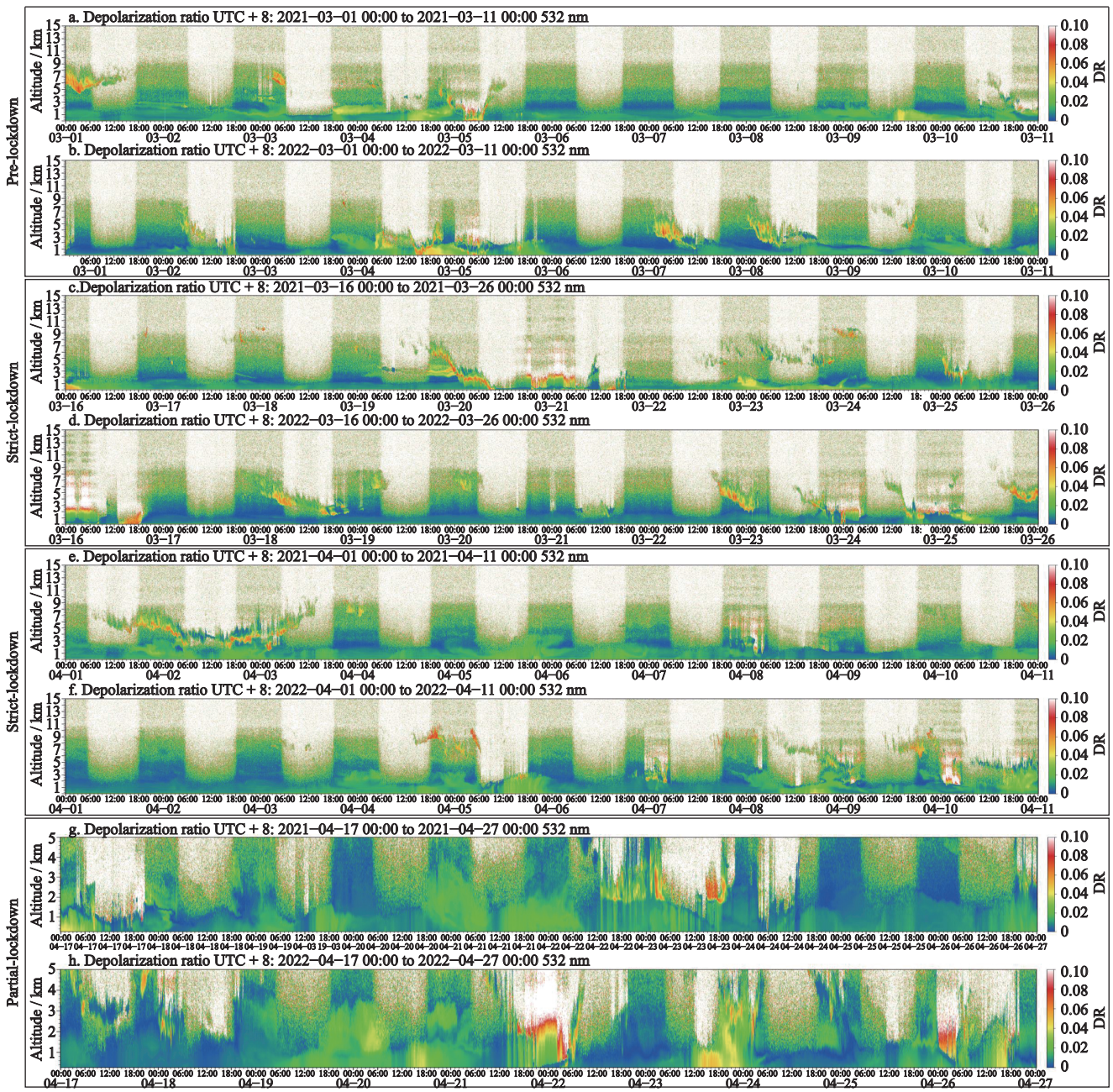

Fig. 3 Vertical profiles of depolarization ratio at sub-minute scales during different stages of lockdown in Changchun City, China in 2022 and for the same periods in 2021. DR, Detection and Ranging

notable difference of DR between 2021 and 2022 can be seen in the near-surface DR in April (Figs. 3c−3h), which was associated with more dust events of aerosol pollution occurred in April 2022. The dust-aerosol layer reached a height of about 2.5 km and persisted for more than 12 h, as shown in Fig. 3f. During the strict lockdown in March 2022, the average DR within 0–5 km was 0.075, an increase of 34.8% over the same period in the previous year. During the partial lockdown period, although more dust events occurred, the DR fell by 14.3% and averaged 0.116. Typically, the DR of dust particles is greater than 0.2, while the DR of anthropogenically contaminated aerosols was less than 0.1 (Xie et al., 2008; Nemuc et al., 2013). According to a previous study (Tian et al., 2017), the regional mean DR in Northeast China during previous spring seasons was greater than that in other seasons, with a mean above 0.1. Furthermore, the particle DR of dust aerosols in East China decreased by 40.3% during the lockdown period in 2021 compared to the same period in 2018 (Chen et al., 2021). This implies that the optical properties of aerosols were significantly reduced during dusty weather due to reduced human activity as a result of COVID-19 control measures.

To exclude the natural influence of sandstorms and to explore the link between human activities and aerosols, we omitted the parts of the data set that were related to dust particles (DR > 0.2). The resulting vertical distribution of the aerosol EC obtained from the ground-based LiDAR data set during the day (06:00–18:00) is shown in Fig. 4. The maximum value of the average EC occurred at the lowest detectable height, which ranged

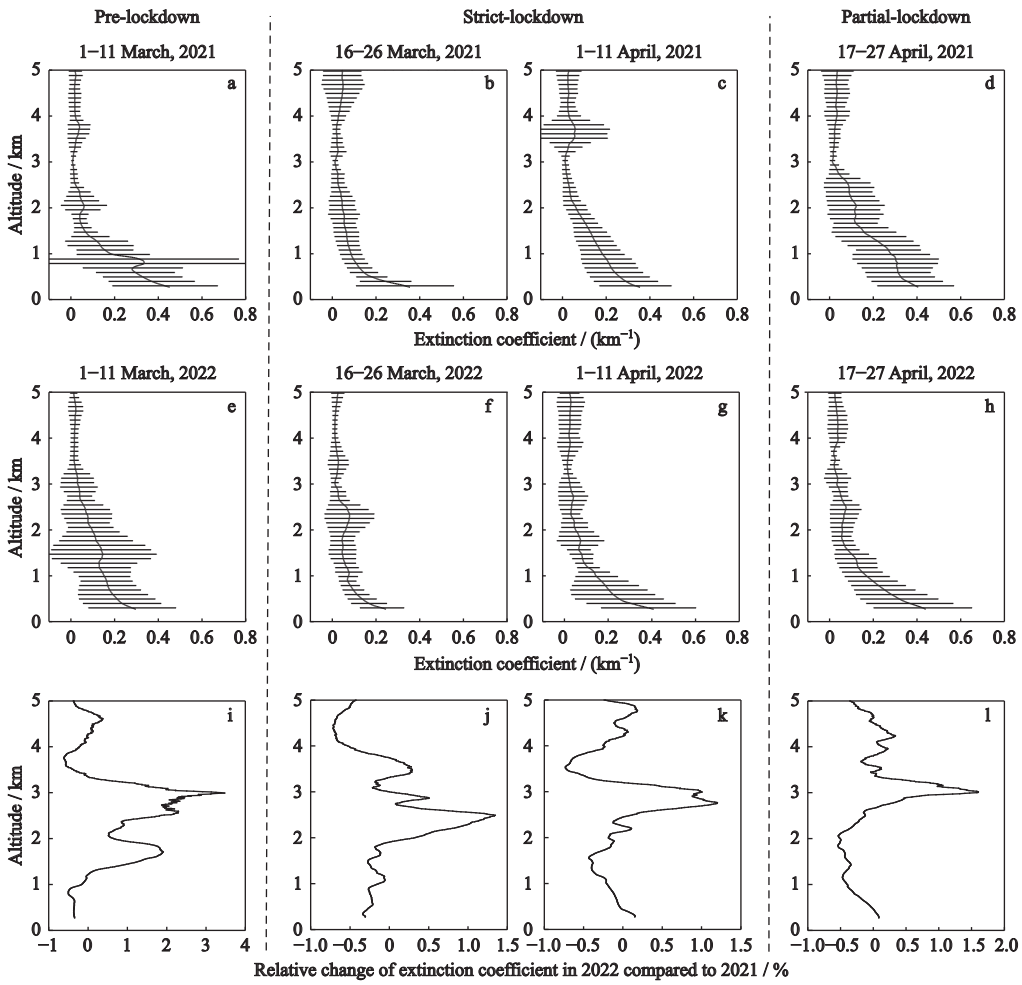

Fig. 4 Vertical distributions of extinction coefficient with the removal of sandy weather conditions for the pre-lockdown, strict lockdown, and partial lockdown periods in Changchun City, China in 2022 and for the same periods in 2021. The curves represent the mean extinction coefficient for each period and the horizontal lines represent the standard deviations of extinction coefficient (a–h). Black curves indicate the relative changes in extinction coefficient in 2022 compared to that in 2021 (i–l)

from 0.2 to 0.4 km^{-1}. During the strict lockdown period in 2022, the mean EC at 0–2 km altitude decreased by 42.7% compared to the pre-lockdown period and by 0.02 (15.0%) compared to the same period in 2021. The EC values within 2 km during the lockdown were significantly lower than those during the same period last year (Figs. 4j and 4k). Following the exclusion of dust aerosols, we observed that the range of ECs within 2 km altitude for all periods in 2022 was smaller than that in 2021. This suggests that the lockdown was effective in mitigating particulate aerosol pollution in the near-surface layer. These findings help deepen the understanding of the relationship between anthropogenic controls and aerosol pollution, and they provide scientific support to governments for developing pollution-control plans.

4 Conclusions

Changchun, the Chinese city that was intensely affected by COVID-19 in 2022, was closed for nearly two months, drastically reducing the intensity of emissions from anthropogenic sources (e.g., mobile and industrial sources). During the strict lockdown period, the surface concentration of NO_2 decreased by more than 61%, particulate matter decreased by 41%, ozone increased slightly, and the EC in the vertical profile of particulate matter decreased by 11%–33%. These changes in air pollutants during this period provide an indication of the potential for urban air-quality improvement. However, with the resumption of production by key industrial enterprises and agricultural activities, especially straw burning, the concentrations of surface particulate matter and the vertical EC increased significantly, by 37%–69%, during the partial lockdown period, indicating the importance of management and control of open burning of straw in spring. This provides a scientific basis for further improvements in air quality in the region.

References

Benchrif A, Wheida A, Tahri M et al., 2021. Air quality during three covid-19 lockdown phases: AQI, $PM_{2.5}$ and NO_2 assessment in cities with more than 1 million inhabitants. *Sustainable Cities and Society*, 74: 103170. doi: 10.1016/j.scs.2021.103170

Bhawar R L, Fadnavis S, Kumar V et al., 2021. Radiative impacts of aerosols during COVID-19 lockdown period over the Indian region. *Frontiers in Environmental Science*, 9: 746090. doi: 10.3389/fenvs.2021.746090

Chen B, Huang Y, Huang J P et al., 2021. Using Lidar and historical similar meteorological fields to evaluate the impact of anthropogenic control on dust weather during COVID-19. *Frontiers in Environmental Science*, 9: 806094. doi: 10.3389/fenvs.2021.806094

Chen W W, Tong D Q, Zhang S C et al., 2017. Local PM_{10} and $PM_{2.5}$ emission inventories from agricultural tillage and harvest in northeastern China. *Journal of Environmental Sciences*, 57: 15–23. doi: 10.1016/j.jes.2016.02.024

Collivignarelli M C, Abbà A, Bertanza G et al., 2020. Lockdown for CoViD-2019 in Milan: what are the effects on air quality. *Science of the Total Environment*, 732: 139280. doi: 10.1016/j.scitotenv.2020.139280

Fernald F G, 1984. Analysis of atmospheric lidar observations: some comments. *Applied Optics*, 23(5): 652–653. doi: 10.1364/AO.23.000652

Fu J, Song S T, Guo L et al., 2022. Interprovincial joint prevention and control of open straw burning in Northeast China: implications for atmospheric environment management. *Remote Sensing*, 14(11): 2528. doi: 10.3390/rs14112528

Gobbi G P, Barnaba F, Giorgi R et al., 2000. Altitude-resolved properties of a Saharan dust event over the Mediterranean. *Atmospheric Environment*, 34(29–30): . doi: 10.1016/S1352-2310(00)00194-1

He J J, Gong S L, Yu Y et al., 2017. Air pollution characteristics and their relation to meteorological conditions during 2014–2015 in major Chinese cities. *Environmental Pollution*, 223: 484–496. doi: 10.1016/j.envpol.2017.01.050

Hua J X, Zhang Y X, de Foy B et al., 2021. Quantitative estimation of meteorological impacts and the COVID-19 lockdown reductions on NO_2 and $PM_{2.5}$ over the Beijing area using generalized additive models (GAM). *Journal of Environmental Management*, 291: 112676. doi: 10.1016/j.jenvman.2021.112676

Li B, Shi X F, Liu Y P et al., 2020. Long-term characteristics of criteria air pollutants in megacities of Harbin-Changchun megalopolis, Northeast China: spatiotemporal variations, source analysis, and meteorological effects. *Environmental Pollution*, 267: 115441. doi: 10.1016/j.envpol.2020.115441

Lian X B, Huang J P, Huang R J et al., 2020. Impact of city lockdown on the air quality of COVID-19-hit of Wuhan city. *Science of the Total Environment*, 742: 140556. doi: 10.1016/j.scitotenv.2020.140556

Liu Z, Wang R N, Liu Z T, 2022. Research on the satisfaction degree characteristics of residential public resources under lockdowns for pandemic prevention and control: a case study in the Changchun. *Sustainability*, 14(8): 4385. doi: 10.3390/su14084385

Lu Chengwei, Fu Jing, Liu Xiufen et al., 2021. Air pollution and meteorological conditions significantly contribute to the worsening of allergic conjunctivitis: a regional 20-city, 5-year study in Northeast China. *Light:Science & Applications*, 10:

190. doi: 10.1038/s41377-021-00630-6

Murayama T, Okamoto H, Kaneyasu N et al., 1999. Application of lidar depolarization measurement in the atmospheric boundary layer: effects of dust and sea-salt particles. *Journal of Geophysical Research:Atmospheres*, 104(D24): 31781–31792. doi: 10.1029/1999JD900503

Nakada L Y K, Urban R C, 2020. COVID-19 pandemic: impacts on the air quality during the partial lockdown in São Paulo state, Brazil. *Science of the Total Environment*, 730: 139087. doi: 10.1016/j.scitotenv.2020.139087

Nemuc A, Vasilescu J, Talianu C et al., 2013. Assessment of aerosol's mass concentrations from measured linear particle depolarization ratio (vertically resolved) and simulations. *Atmospheric Measurement Techniques*, 6(11): 3243–3255. doi: 10.5194/amt-6-3243-2013

Sharma S, Zhang M Y, Anshika et al., 2020. Effect of restricted emissions during COVID-19 on air quality in India. *Science of the Total Environment*, 728: 138878. doi: 10.1016/j.scitotenv.2020.138878

Shen Z X, Cao J J, Arimoto R et al., 2007. Chemical composition and source characterization of spring aerosol over Horqin sand land in northeastern China. *Journal of Geophysical Research:Atmospheres*, 112(D14): D14315. doi: 10.1029/2006JD007991

Thomas A, Kanawade V P, Sarangi C et al., 2021. Effect of COVID-19 shutdown on aerosol direct radiative forcing over the Indo-Gangetic Plain outflow region of the Bay of Bengal. *Science of the Total Environment*, 782: 146918. doi: 10.1016/j.scitotenv.2021.146918

Tian P F, Cao X J, Zhang L et al., 2017. Aerosol vertical distribution and optical properties over China from long-term satellite and ground-based remote sensing. *Atmospheric Chemistry and Physics*, 17(4): 2509–2523. doi: 10.5194/acp-17-2509-2017

Tobías A, Carnerero C, Reche C et al., 2020. Changes in air quality during the lockdown in Barcelona (Spain) one month into the SARS-CoV-2 epidemic. *Science of the Total Environment*, 726: 138540. doi: 10.1016/j.scitotenv.2020.138540

Wang P, Che H Z, Zhang X C et al., 2010. Aerosol optical properties of regional background atmosphere in Northeast China. *Atmospheric Environment*, 44(35): 4404–4412. doi: 10.1016/j.atmosenv.2010.07.043

Wang X M, Dong Z B, Zhang J W et al., 2004. Modern dust storms in China: an overview. *Journal of Arid Environments*, 58(4): 559–574. doi: 10.1016/j.jaridenv.2003.11.009

Xie C B, Nishizawa T, Sugimoto N et al., 2008. Characteristics of aerosol optical properties in pollution and Asian dust episodes over Beijing, China. *Applied Optics*, 47(27): 4945–4951. doi: 10.1364/AO.47.004945

Yin Z P, Yi F, Liu F C et al., 2021. Long-term variations of aerosol optical properties over Wuhan with polarization lidar. *Atmospheric Environment*, 259: 118508. doi: 10.1016/j.atmosenv.2021.118508

Zangari S, Hill D T, Charette A T et al., 2020. Air quality changes in New York City during the COVID-19 pandemic. *Science of the Total Environment*, 742: 140496. doi: 10.1016/j.scitotenv.2020.140496

Zhao H J, Gui K, Ma Y J et al., 2022. Effects of different aerosols on the air pollution and their relationship with meteorological parameters in North China Plain. *Frontiers in Environmental Science*, 10: 814736. doi: 10.3389/fenvs.2022.814736